Mechanism of Cytochrome *c* Oxidase-Catalyzed Reduction of Dioxygen to Water: Evidence for Peroxy and Ferryl Intermediates at Room Temperature†

Artur Sucheta, Katy E. Georgiadis,‡ and Ólöf Einarsdóttir*

Department of Chemistry and Biochemistry, University of California, Santa Cruz, California 95064

Received September 25, 1996; Revised Manuscript Received November 13, 1996⊗

ABSTRACT: The reaction between bovine heart cytochrome oxidase and dioxygen was investigated at room temperature following photolysis of the fully reduced CO-bound enzyme. Time-resolved optical absorption difference spectra were collected by a gated multichannel analyzer in the visible region (λ = 460−720 nm) from 50 ns to 50 ms after photolysis. Singular value decomposition (SVD) analysis indicated the presence of at least seven intermediates. Multiexponential fitting gave the following apparent lifetimes: 1.2 μs, 10 μs, 25 μs, 32 μs, 86 μs, and 1.3 ms. On the basis of the SVD results and a double difference map, a sequential kinetic mechanism is proposed from which the spectra and time-dependent populations of the reaction intermediates were determined. The ferrous-oxy complex (compound A), with a peak at 595 nm and a trough at 612 nm versus the reduced enzyme, reaches a maximum concentration ∼30 μs after photolysis. It decays to a 1:6 mixture of peroxy species (a_3^{3+}-O^--O^-) in which cytochrome *a* is reduced and oxidized. Cytochrome a_3 in both species has a peak at 606 nm versus its oxidized form. The peroxy species decay to a ferryl intermediate, with a peak at 578 nm versus the oxidized enzyme, followed by electron redistribution between Cu_A and cytochrome *a*. The two ferryl species reach a maximum concentration ∼310 μs after photolysis. The excellent agreement between the experimental and theoretical spectra of the intermediates provides unequivocal evidence for the presence of peroxy and ferryl species during dioxygen reduction by cytochrome oxidase at room temperature.

The reactions of partially or fully reduced cytochrome *c* oxidase with dioxygen are so fast that conventional stopped-flow methods are impractical. Therefore, these reactions have usually been studied by the flow-flash technique developed by Greenwood and Gibson (Gibson & Greenwood, 1963; Greenwood & Gibson, 1967) in which carbon monoxide is photodissociated from the CO complex of either the fully reduced or the mixed-valence enzyme in the presence of O_2 [see Einarsdóttir (1995) for a recent review]. Time-resolved optical absorption (TROA)[1] studies have provided information about the kinetics of the internal electron transfer processes (Hill & Greenwood, 1984; Orii, 1988a; Oliveberg et al., 1989; Hill, 1994; Verkhovsky et al., 1994) and, more recently, spectral characteristics (Morgan et al., 1996). Low-temperature optical absorption experiments (Chance et al., 1975; Clore et al., 1980) and EPR studies (Karlsson et al., 1981; Hansson et al., 1982; Blair et al., 1985; Witt et al., 1986; Witt & Chan, 1987) have also yielded useful information about some of the transient intermediates generated during dioxygen reduction. By use of evidence from time-resolved resonance Raman (TR^3) spectroscopy (Han et al., 1990a; Ogura et al., 1993; Varotsis et al., 1993), the structures of some of the intermediates formed during the reaction have been proposed. However, the microscopic rate constants of all the steps involved and the existence and nature of other intermediates, including their optical absorption spectra, have not been reported at room temperature.

Previous single-wavelength flow-flash TROA studies indicated the presence of four processes during the reaction of the fully reduced enzyme with dioxygen (Oliveberg et al., 1989). The first step with an apparent lifetime, τ, of 8−10 μs has generally been attributed to the binding of O_2 to the ferrous cytochrome a_3, forming the so-called compound A (Oliveberg et al., 1989; Verkhovsky et al., 1994). This intermediate has been detected in low-temperature optical absorption measurements (Chance et al., 1975; Clore et al., 1980; Morgan et al., 1996) and at room temperature by TR^3 spectroscopy (Varotsis et al., 1989; Ogura et al., 1990a; Han et al., 1990b). However, the optical absorption spectrum of compound A has not been reported at room temperature.

The second process with τ of 32−45 μs has generally been attributed to the formation of a peroxy species in which both

† This work was supported by National Institutes of Health Grant GM45888.

* Author to whom correspondence should be addressed: e-mail, olof@chemistry.ucsc.edu; fax, 408-459-2935.

‡ Present address: Department of Chemistry, Baker Laboratory, Cornell University, Ithaca, NY 14853.

⊗ Abstract published in *Advance ACS Abstracts,* January 1, 1997.

[1] Abbreviations: SVD, singular value decomposition; OSMA, optical spectrometric multichannel analyzer; **b**-spectrum, spectral changes associated with a particular first-order process; **u**-spectra, the orthonormal basis spectra represented by the *n* columns of the **U** matrix; **v**-vectors, the *n* columns of the **V** matrix describing the time evolution of the **u**-spectra; TROA, time-resolved optical absorption; TR^3, time-resolved resonance Raman; EPR, electron paramagnetic resonance; τ, apparent lifetime; Cu_A, the mixed-valence copper A center; Cu_B, copper B; a^{2+}, reduced cytochrome *a*; a^{3+}, oxidized cytochrome *a*; a_3^{2+}, reduced cytochrome a_3; a_3^{3+}, oxidized cytochrome a_3; compound A, the ferrous-oxy complex of cytochrome a_3; P, a form of the enzyme in which both cytochrome a_3 and Cu_B are oxidized and cytochrome a_3 has an absorbance maximum at ∼607 nm when referenced against its oxidized state; P′, a form of the enzyme in which both cytochrome *a* and a_3 are oxidized, Cu_B is reduced, and cytochrome a_3 has an absorbance maximum at ∼607 nm when referenced against its oxidized state; F, a form of the enzyme in which cytochrome a_3 has an absorbance maximum at ∼580 nm when referenced against its oxidized state; F_I, form F in which cytochrome *a* is oxidized; F_{II}, form F in which cytochrome *a* is reduced.

S0006-2960(96)02422-1 CCC: $14.00

hemes become oxidized and Cu_B is reduced (hereafter referred to as P′) (Hill & Greenwood, 1984; Han et al., 1990c; Hill, 1994; Verkhovsky et al., 1994; Morgan et al., 1996). Another peroxy compound, P, in which the binuclear center is oxidized and cytochrome *a* remains reduced has been postulated to form prior to the oxidation of cytochrome *a* (Babcock & Wikström, 1992; Varotsis et al., 1993). Neither P nor P′ has been detected by room-temperature TROA or TR[3] measurements during the reaction of the fully reduced enzyme with dioxygen, the former presumably due to its low occupancy. However, a species is observed during the reversal of the dioxygen reduction reaction that is 2 equiv more oxidized than the resting enzyme and has an absorbance maximum at 607 nm when referenced against the oxidized enzyme (Wikström & Morgan, 1992). This species was attributed to a peroxy form of cytochrome a_3 (a_3^{3+}-O^--O^-, Cu_B^{2+}), P. A species with a maximum at 607 nm when referenced against the oxidized enzyme is also observed when the oxidized enzyme is exposed to a mixture of CO and O_2 or upon addition of hydrogen peroxide to the oxidized enzyme (Bickar et al., 1982; Wrigglesworth, 1984; Vygodina & Konstantinov, 1988; Fabian & Palmer, 1995b). A species with similar spectral properties has been observed when the mixed-valence enzyme reacts with oxygen at low temperature (Chance et al., 1975; Clore et al., 1980) and room temperature (Hill & Greenwood, 1983; Han et al., 1990d). Morgan et al. (1996) have recently shown by transient optical absorption measurements that a 607-nm species, equivalent to P′, is formed at −25 °C during the reaction of the fully reduced cytochrome oxidase with dioxygen.

The third phase with τ of 100−140 μs (Hill & Greenwood, 1984; Oliveberg et al., 1989; Hill, 1994) has been associated with the oxidation of Cu_A (Hill, 1991). On a similar or slightly slower time scale, a ferryl, F (a_3^{4+}═O), intermediate is formed. This is supported by TR[3] measurements which suggested that F reaches a maximum concentration ∼500 μs following CO photolysis (Varotsis et al., 1993). A species with an absorbance maximum at 580 nm (referenced against the oxidized enzyme) is observed when a one-electron reversal of the dioxygen reduction reaction is induced (Wikström & Morgan, 1992) and for the three-electron-reduced dioxygen intermediate at low temperature (Witt et al., 1986; Witt & Chan, 1987). Both species were identified as F. An optical absorption evidence for the formation of F concomitant with electron transfer from Cu_A to cytochrome *a* has recently been reported at −25 °C (Morgan et al., 1996). The formation of F at room temperature is supported by peaks at 575 and 530 nm in the 100-μs minus 20-μs optical absorption difference spectrum (Orii, 1988a).

The last phase of dioxygen reduction with τ of ∼1.2 ms is attributed to further reduction by one electron. Schemes encompassing other intermediates, including proton transfers, have also been proposed (Babcock & Wikström, 1992; Einarsdóttir, 1995; Varotsis & Babcock, 1995).

In the study reported here, we used a gated optical spectrometric multichannel analyzer (OSMA) to detect spectral changes occurring during the reaction of dioxygen with cytochrome oxidase at room temperature following photolysis of the fully reduced CO complex. This allows us to collect high-resolution (0.3−0.6 nm) spectra with a temporal resolution of several nanoseconds. Spectral changes were monitored in the visible region (λ = 470−720 nm) from 50 ns to 50 ms following photolysis. After singular value decomposition (SVD) and global analysis of the spectra, a kinetic mechanism involving a sequential pathway with accompanying equilibria was fitted to the data. On the basis of this pathway, we obtained the spectra of the intermediates, including compound A and peroxy and ferryl species, with absorbance maxima at 606 and 578 nm, respectively.

MATERIALS AND METHODS

Cytochrome oxidase was isolated from bovine heart tissue using the method of Yoshikawa et al. (1977). The final dialysis was against 0.1 M sodium phosphate buffer, pH = 7.4. Sodium L-ascorbate was obtained from Sigma, and ruthenium hexaammine chloride [hexaammineruthenium(II) chloride] was from Alfa Products (Johnson Matthey, Danver, MA). Both reagents were used without further purification.

The fully reduced enzyme was made by deoxygenating a solution of oxidized enzyme with several alternating cycles of gentle vacuum and prepurified N_2 gas, followed by the addition of anaerobic solutions of 2.5 M ascorbate and 200 mM ruthenium hexaammine. The final concentrations of ascorbate and ruthenium hexaammine in the enzyme solution were 1.0−5.0 mM and 5−500 μM, respectively. The fully reduced CO-bound complex was obtained by passing a 1-atm mixture of CO and N_2 in a ratio of 1:9 over a solution of the fully reduced enzyme solution for 30−60 min. The complex was kept under this mixture during the experiment. At each stage of the preparation, the UV−visible spectra of the oxidized, fully reduced, and the fully reduced CO complexes were recorded. Enzyme concentration was determined spectrophotometrically using extinction coefficients of 79.6 mM^{-1} cm^{-1} (420 nm) and 8.5 mM^{-1} cm^{-1} (598 nm) for the fully oxidized enzyme and 106.4 mM^{-1} cm^{-1} (444 nm) and 19.9 mM^{-1} cm^{-1} (604 nm) for the reduced enzyme (Yoshikawa et al., 1977; Antalis & Palmer, 1982). The concentration of cytochrome oxidase, equal to half the heme A concentration, was 17 μM after mixing.

The reaction of the fully reduced enzyme with oxygen was investigated at room temperature using the flow-flash method (Greenwood & Gibson, 1967). Solutions of O_2-saturated (1.25 mM) phosphate buffer (0.1 M, pH 7.4) and the fully reduced CO enzyme complex in the same buffer but saturated with CO/N_2 (1:9) were mixed in a 1:1 ratio in a 80-μL flow cell (10 × 2 × 4 mm, lwh) by a syringe pump actuated with a stepper motor. The flow cell was an integral part of the RX1000 rapid kinetics accessory (Applied Photophysics) stopped-flow apparatus. The flow cell was thermostated to 298.2 ± 0.4 K during all experiments. Following a post-mixing delay of 400 ms, the reaction was initiated by photolyzing the CO complex with a DCR-11 Nd:Yag laser (Quanta-Ray) (532 nm, 45 mJ/pulse). The photolytic efficiencies measured under identical conditions in the absence of O_2 were ∼60%. The spectral changes were probed along the 10-mm path at 90° to the laser photolyzing beam. The light source was a pulsed xenon flashlamp, and appropriate filters restricted the probe beam to the spectral region of interest. The energy of the probe beam was low enough that it did not photodissociate the CO complex. Each spectrum (one time point) was an average of 18 runs. Light transmitted through the sample was passed through collimating optics (fused silica lenses) and then focused onto the entrance slit of a spectrograph (Aries, FF250). The signals

were detected by an intensified gated optical spectrometric multichannel analyzer (OSMA) (I/R/Y, Princeton Instruments) system described earlier (Georgiadis et al., 1994; Einarsdóttir et al., 1995).

Singular Value Decomposition and Global Exponential Fitting. Time-resolved absorption difference spectra (post-minus prephotolysis) were measured at 42 delay times (defined exponentially) between 50 ns and 50 ms following the laser pulse. The transient difference spectra were corrected by subtracting background counts from the detector from the observed intensities. The time-resolved difference spectra constitute a two-dimensional (wavelength × delay) data matrix, $\Delta\mathbf{A}$ (λ_m, t_n), where m and n are the number of wavelengths and times collected, respectively. The $\Delta\mathbf{A}$ matrix was analyzed using Matlab software (The MathWorks) at all wavelengths and times simultaneously by singular value decomposition (SVD) as described previously (Georgiadis et al., 1994; Einarsdóttir et al., 1995). In this analysis, three matrices **U**, **S**, and **V** are generated such that $\Delta\mathbf{A} = \mathbf{USV}'$. The n columns of the **U** matrix are the orthonormal basis spectra (**u**-spectra), the diagonal **S** matrix ($n \times$ n) contains the corresponding singular values, and each column of the ($n \times n$) **V** matrix (**v**-vector) describes the time evolution of the corresponding **u**-spectrum (Golub & Reinsch, 1970; Henry & Hofrichter, 1992). $\mathbf{V}'$ is the transpose of **V**. A semilogarithmic plot of the singular values in conjunction with plots of the **u**-spectra and the **v**-vectors was used to evaluate the minimum number of processes required to represent the $\Delta\mathbf{A}$ matrix. The **U** and **V** matrices were subsequently truncated to include only columns whose singular values exceeded the experimental noise. A sum of exponentials was globally fitted by nonlinear regression to the **v**-vectors of the resultant reduced data set (Hug et al., 1990; Thorgeirsson et al., 1991, 1992).

Further analysis involved construction of a smoothed two-dimensional map of the double difference spectra ($\Delta\Delta\mathbf{A}$). The map is plotted as a top view of the surface representing the time-resolved $\Delta\Delta\mathbf{A}$ as a function of log (delay time) and wavelength. The time-resolved $\Delta\Delta\mathbf{A}$ were obtained by subtracting each time-resolved difference spectrum from the preceding spectrum. Mathematically, for an ($m \times n$) $\Delta\mathbf{A}$ matrix, $\Delta\Delta\mathbf{A}$ is defined as

$$\Delta\Delta\mathbf{A}_{i,j} = \Delta\mathbf{A}_{i,j} - \Delta\mathbf{A}_{i,j-1}$$

where $i = 1, ..., m$ and $j = 2, ..., n$. Smoothing involved a two-dimensional variation of the boxcar algorithm, according to

$$\Delta\Delta\mathbf{A}^{\mathrm{sm}}_{i,j} = \{\sum_{\alpha=i-1}^{i+1}\sum_{\beta=j-1}^{j+1}\Delta\Delta\mathbf{A}_{\alpha,\beta} - \Delta\Delta\mathbf{A}_{i,j}\}/8$$

where $\Delta\Delta\mathbf{A}^{\mathrm{sm}}_{i,j}$ is the smoothed double difference matrix. The double difference map and the results of the SVD, i.e., the **u**-spectra and the **v**-vectors, were used to obtain unbiased information from the data, including the number of detectable intermediates (as indicated by the above-the-noise singular values) and correlations between spectral and temporal changes.

In the next stage of the analysis, nonlinear regression fitting was used to determine the apparent lifetimes of the observed processes and the associated spectral changes, the **b**-spectra. The rank of the $\Delta\mathbf{A}$ matrix was determined from the number of nonrandom **uv** couples resulting from the SVD. In the course of the regression analysis, the number of exponentials used was increased until no further improvement was observed in the residual spectra (the difference between the transient data and the fit). The results of the SVD, the double difference map, and the exponential fitting were used to construct a kinetic mechanism.

Kinetic Modeling. The goal of our analysis is to extract the spectra of the intermediates predicted by a particular mechanism and a set of microscopic rate constants. As pointed out in our previous papers, the global fitting routine using SVD gives only information about the apparent variables, the **b**-spectra and their corresponding apparent rate constants (Georgiadis et al., 1994; Einarsdóttir et al., 1995). Only for a simple unidirectional scheme are the apparent rate constants equal to the microscopic rate constants. If any of the reaction steps are reversible, as is the case here, the number of variables exceeds the number of constraints and the kinetic matrix comprising the microscopic rate constants becomes undetermined. This problem is tractable if spectra of at least some of the intermediates are known. In this study the microscopic rate constants were based on published data when available, but the final values were refined by varying the constants iteratively in a simplex optimization algorithm until the calculated apparent lifetimes did not depart from the experimental ones and the difference spectra of the extracted intermediates (experimental spectra) resembled theoretical difference spectra. The theoretical difference spectra for the various intermediates were the linear combinations of the ground-state absorbance spectra of the oxidized, reduced, mixed-valence CO, and fully reduced CO enzyme complexes and the peroxy and ferryl derivatives. The peroxy ($a_3{}^{3+}$-O-O$^-$) and ferryl ($a_3{}^{4+}$=O) species, with maxima at 606 and 580 nm when referenced against the oxidized enzxyme, were synthesized according to previously described methods (Fabian & Palmer, 1995a). The concentrations of P and F were calculated on the basis of their difference spectra using extinction coefficients of 11 mM^{-1} cm^{-1} at 607−630 nm and 5.3 mM^{-1} cm^{-1} at 580−630 nm, respectively (Wikström & Morgan, 1992).

RESULTS

The transient absorption difference spectra following photolysis of the fully reduced CO complex in the presence of oxygen are shown in Figure 1. The spectra represent the difference between the photoproducts and the fully reduced CO complex at 42 delay times between 50 ns and 50 ms. Several experiments included time delays between 50 ms and 500 ms, but since only minor changes were observed in the transient difference spectra during this time interval, these data points were omitted. The difference spectrum observed at 50 ns has a peak at 618 nm and a trough at 592 nm and is identical to the one obtained in the absence of O_2. The final difference spectrum recorded at 50 ms is similar (although not identical) to the difference spectrum of the fully oxidized enzyme.

Double Difference Map and Singular Value Decomposition. The experiments carried out in the visible region extend in time over 6 orders of magnitude. Figure 2 shows a double difference map obtained as the top view of a three-dimensional plot representing the time-resolved $\Delta\Delta\mathbf{A}$ as a function of log (time) and wavelength. The rates of absorbance decrease and increase are indicated by darker

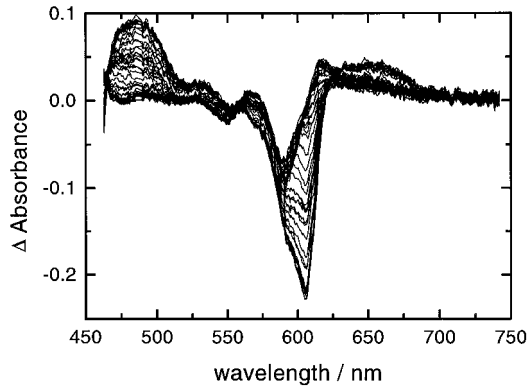

FIGURE 1: Time-resolved absorption difference spectra (post- minus prephotolysis) collected during the reaction of the fully reduced cytochrome oxidase with dioxygen. The spectra were obtained at 42 delay times, defined exponentially, between 50 ns and 50 ms after photolysis of the fully reduced CO complex. Each spectrum represents the average of 18 accumulations. The cytochrome oxidase concentration after mixing was 17.0 ± 1.5 μM in 0.1 M sodium phosphate buffer (pH = 7.4) at 24 °C. The CO and O_2 concentrations after mixing were 50 and 625 μM, respectively.

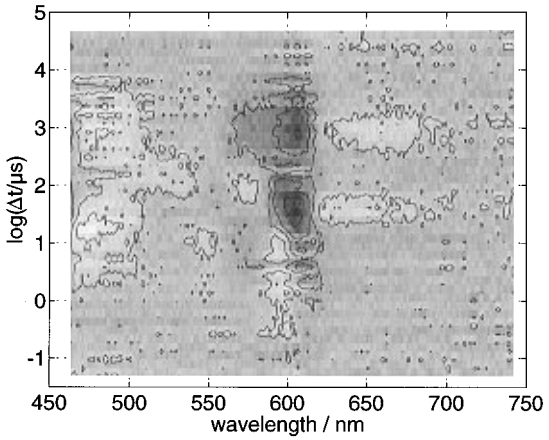

FIGURE 2: Smoothed double difference map (the top view of a three-dimensional plot representing the time-resolved double difference spectra, $\Delta\Delta\mathbf{A}$) as a function of log (delay time) and wavelength. The smoothed double difference spectra were obtained by subtracting each time-resolved difference spectrum from the preceding spectrum (see text for details). The rates of absorbance decrease and increase are indicated by darker and lighter shadings, respectively.

and lighter shadings, respectively. The double difference map, along with SVD results, provides qualitative information regarding correlations between spectral and temporal changes from which a mechanism for the dioxygen reduction reaction can be proposed. Figure 3 shows the first six **u**-spectra and the corresponding **v**-vectors resulting from the SVD of the transient difference spectra referenced against the spectrum of the oxidized enzyme. The remaining **uv** couples did not have signal-to-noise ratio exceeding the experimental noise. The experimental **v**-vectors were modeled using the observed apparent lifetimes (see below). Although each **uv** couple represents a combination of spectral changes and time evolution of several processes, inspection of these vectors provides qualitative information about the data. The clearest correlations between spectral and temporal changes are the following:

(i) For reaction times shorter than 1 μs, only minor changes are observed in all the **v**-vectors except **v5**, which contains information about a ~1-μs process (Figure 3). The largest changes in the transient difference spectra at this time occur at 603 and 612 nm as reflected in **u5**. These spectral and temporal changes are in agreement with those observed following photolysis of the fully reduced CO-bound enzyme in the absence of O_2. Small deviation from the average (gray) shade can be observed in the $\Delta\Delta\mathbf{A}$ map (Figure 2) on the same time scale.

(ii) Spectral changes that follow this short time scale process are reflected by a rise in absorbance at ~595 and 550 nm and an absorbance decrease at ~570 and ~610 nm in the $\Delta\Delta\mathbf{A}$ map between 1 and 20 μs. The same spectral changes are reflected in the **u2** spectrum, and the **v2** vector indicates that the corresponding species reaches a maximum concentration ~30 μs after photolysis. These spectral changes are similar to those observed for the mixed-valence CO-bound enzyme in low temperature triple trap experiments (Chance et al., 1975; Clore et al., 1980) and room-temperature flow-flash experiments (Hill & Greenwood, 1983), which were assigned to the binding of O_2 to cytochrome a_3. The binding of O_2 to the ferrous cytochrome a_3 on this time scale is also consistent with room-temperature flow-flash TROA results on the fully reduced enzyme (Greenwood & Gibson, 1967; Orii, 1984; Oliveberg et al., 1989; Blackmore et al., 1991; Verkhovsky et al., 1994) and TR^3 data (Varotsis et al., 1989; Ogura et al., 1990a; Han et al., 1990b).

(iii) The **u1** spectrum, with an absorbance maximum at 605 nm (Figure 3), resembles the fully reduced-minus-oxidized difference spectrum. Since cytochrome a_3 has a small contribution to this difference spectrum in the visible region, the spectral changes in **u1** primarily reflect changes in the redox state of cytochrome *a*. The **v1** vector shows a two-phase decay on time scales of ~30 μs and 1.3 ms, reflecting the oxidation of cytochrome *a* at different times during the reaction cycle. This conclusion is supported by the $\Delta\Delta\mathbf{A}$ map, which shows a sharp absorbance decrease between 30 and 70 μs and again at ~1 ms (Figure 2). The initial oxidation of cytochrome *a* may also be reflected in the fourth **uv** couple, which shows a species with a maximum centered at ~605 nm decaying with an apparent lifetime of ~40 μs (the first portion of **v4**).

(iv) Near 100 μs, an absorbance increase is visible at ~580 nm in the $\Delta\Delta\mathbf{A}$ map, reaching a maximum at ~300 μs. The increase is also observed in the third **uv** couple and is attributed to the formation of F.

(v) These changes are closely followed by a rise in absorbance near 605 nm in the $\Delta\Delta\mathbf{A}$ map, signifying the re-reduction of cytochrome *a*, and an increase in absorbance between 510 and 530 nm, indicative of the oxidation of Cu_A (Einarsdóttir et al., 1995). The very similar time scales of the 580-nm absorbance changes and those at 520 and 605 nm suggest that formation of F is followed by a slightly faster electron redistribution between cytochrome *a* and Cu_A. At ~340 μs, a decrease in absorbance at ~580 nm is observed concomitant with the formation of a saddle point near ~600 nm. The upward portion of **v4** (near ~190 μs) and the corresponding spectral changes at ~605 and 520 nm in **u4** are also consistent with the reduction of cytochrome *a* and the oxidation of Cu_A, respectively.

(vi) The **u6** spectrum due to its low signal-to-noise ratio cannot be interpreted, but it reflects changes near ~580 nm. The significance of the above observations will be addressed in detail in the discussion section.

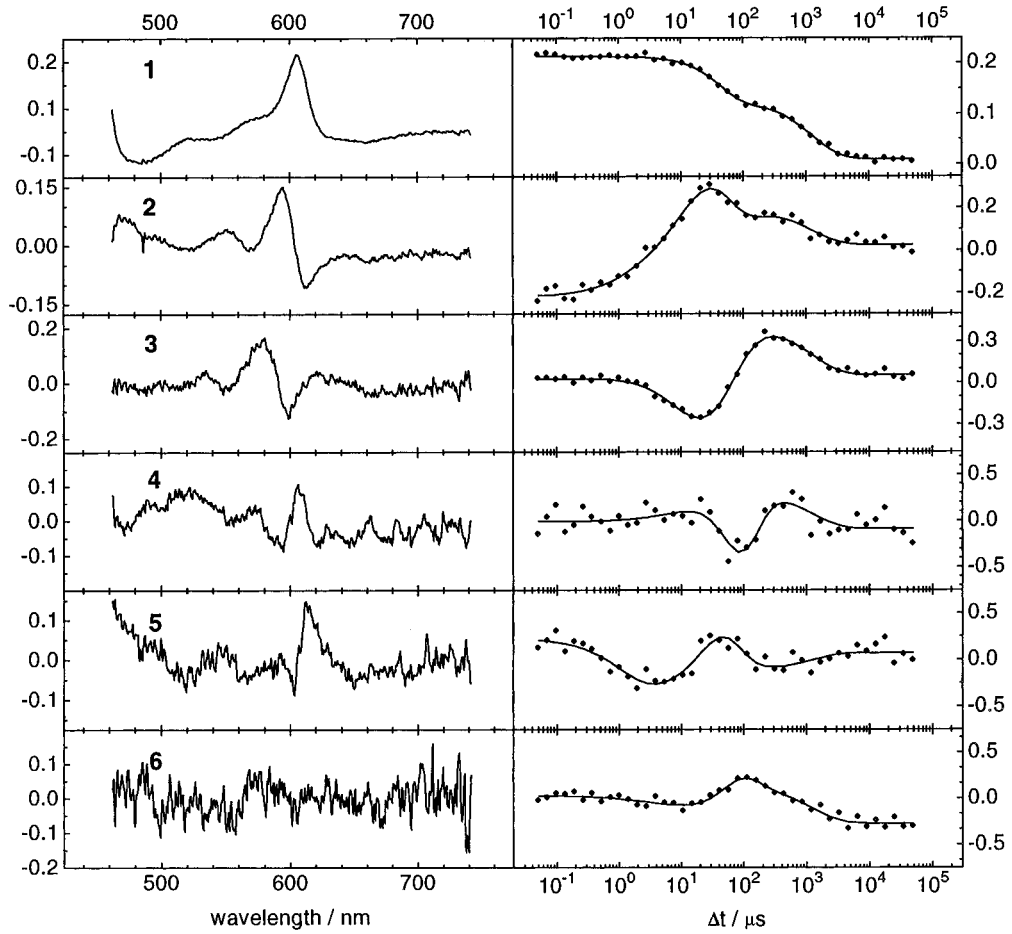

FIGURE 3: First six **u**-spectra (left-hand panels) and **v**-vectors (right-hand panels) resulting from the SVD analysis of the time-resolved difference spectra referenced against the spectrum of the oxidized enzyme. The **v**-vectors (solid lines) are a fit using the apparent lifetimes obtained from the global exponential regression.

Multiexponential Fitting by Nonlinear Regression. The global fitting analysis gave six apparent lifetimes of 1.2 ± 0.2 μs, 10 ± 5 μs, 25 ± 5 μs, 32 ± 5 μs, (86 ± 10 μs, and 1.3 ± 0.1 ms, two more (the 1.2- and 25-μs lifetimes) than reported previously (Oliveberg et al., 1989). The first τ of 1.2 μs is the same as that observed in the absence of O_2 and has been attributed to a conformational change at cytochrome a_3 (Einarsdóttir et al., 1993). Although the two apparent lifetimes, 25 and 32 μs, fall within the experimental error of each other, including both in the analysis significantly improved the residual spectra. Therefore, we believe that both of these lifetimes are real. The residual spectra from the six-exponential fit of the transient difference spectra referenced against the oxidized enzyme are shown in Figure 4. Although the residual spectra are reasonably good, some differences between the data and the fit are observed on ~3-μs and ~10-ms time scales. This suggests the presence of additional intermediates which could not be resolved, presumably due to low occupancy or spectral similarities to adjacent intermediates.

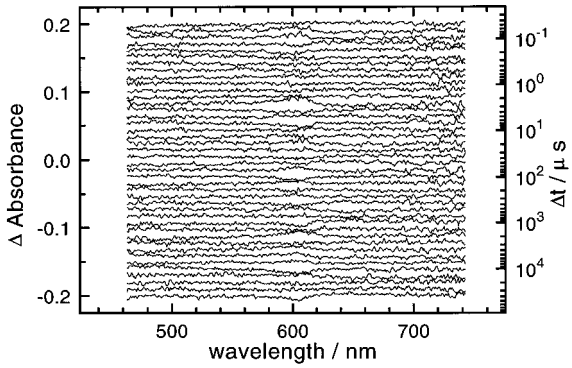

FIGURE 4: Residual spectra (over all the time points plotted in Figure 1) from the six-exponential fit. The lines (from top to bottom) represent the absorbance difference of the data and the least-squares fit at each delay time (defined exponentially) between 50 ns and 50 ms. The residuals have been separated by a constant shift for clarity.

DISCUSSION

A Kinetic Model. The six apparent lifetimes obtained from the multiexponential fitting indicate that at least seven intermediates (including the initial form and the final product) are present on the route from the unliganded reduced enzyme to the oxidized form. Based on the observations from the SVD and the double difference map discussed above, we propose the sequential mechanism in Scheme 1 for the cytochrome oxidase-catalyzed reduction of dioxygen to water. The microscopic rate constants obtained from minimizing a weighted sum of deviations between the experimental and calculated lifetimes and the experimental and theoretical difference spectra of the intermediates are also listed in Scheme 1.

In the first intermediate (1) in Scheme 1, cytochrome a_3 is in an excited-state configuration, possibly related to CO binding to Cu_B (Einarsdóttir et al., 1993). This intermediate subsequently relaxes to the fully reduced unliganded con-

figuration (*R*) on the same time scale that CO dissociates from Cu_B (Dyer et al., 1989). The second step (2 ↔ 3) involves the binding of O_2 to cytochrome a_3, forming compound A. There is considerable experimental evidence that suggests that O_2 binds to Cu_B prior to binding to cytochrome a_3 (Alben et al., 1981; Blackmore et al., 1991; Woodruff et al., 1991; Oliveberg & Malmström, 1992; Einarsdóttir et al., 1993; Bailey et al., 1996), but spectral similarities to intermediate 2 and/or the low occupancy of this state may preclude its optical detection.

The third step in our mechanism (3 ↔ 4) involves the formation of a mixture of two peroxy species (a_3^{3+}-O^--O^-) in a 1:6 ratio, in which cytochrome *a* is reduced (P) and oxidized (P′). Although the peroxide is depicted as being bound only to cytochrome a_3, it is possible that it forms a bridge between cytochrome a_3 and Cu_B. The structure of cytochrome a_3 in both P and P′ is proposed to be equivalent to P observed during reversal of the O_2 reaction (Wikström & Morgan, 1992) and the 607-nm species observed when the resting enzyme is exposed to a mixture of CO and O_2 or substoichiometric amounts of hydrogen peroxide (Bickar et al., 1982; Wrigglesworth, 1984; Vygodina & Konstantinov, 1988; Fabian & Palmer, 1995b). Both P and P′ have been proposed as intermediates in the dioxygen reduction cycle at room temperature (Babcock & Wikström, 1992), and recent optical absorption studies by Morgan et al. (1996) have provided evidence for P′ at −25 °C. However, P′ has not been observed at room temperature, and little supporting evidence is available for P from TROA and TR[3] studies.

The fourth step (4 ↔ 5) involves the formation of a ferryl species (F_I), a_3^{4+}=O Cu_B^{2+}, in which cytochrome *a* remains oxidized. We propose this to be the same F that is formed upon reversal of the O_2 reaction (Wikström & Morgan, 1992) as well as the species formed upon addition of excess hydrogen peroxide to the resting enzyme (Bickar et al., 1982; Fabian & Palmer, 1995a), both of which have an absorbance maximum at 580 nm when referenced against the oxidized enzyme. This step is followed by slightly faster electron redistribution between cytochrome *a* and Cu_A (5 ↔ 6), leading to the formation of F_{II}. The final step involves further reduction by one electron, leading to the formation of a ferric hydroxide, a_3^{3+}-OH. A resonance Raman frequency at 450 cm^{-1} has been assigned to this intermediate (Han et al., 1990b). The residuals resulting from a six-exponential fit to the transient data indicate some deviations around ~8 ms (Figure 4), suggesting that an additional process, presumably the relaxation of the ferric hydroxide to the resting enzyme, occurs on this time scale.

Included in Scheme 1 is the uptake of the protons required during the reduction reaction. We have recently monitored proton uptake in the solubilized enzyme by a pH-sensitive dye (pyranine) and transient optical spectroscopy (Brooks et al., unpublished results). We observed three apparent lifetimes, 100 μs, 1 ms, and 10 ms, the first two being similar to those reported by Hallén and co-workers (Oliveberg et al., 1991; Hallén & Nilsson, 1992). The total number of protons used in the reaction was close to 1.6, with 0.4 proton taken up in each of the 100-μs and 1-ms phases, consistent with earlier observations (Oliveberg et al., 1991), and 0.8 proton taken up in the 10-ms phase. Further proton uptake may occur during the 1-ms phase but is obscured by the simultaneous release of protons on this time scale (Oliveberg et al., 1991). The proton uptake shown in Scheme 1 is based on these observations and those of Hallén and co-workers (Hallén & Nilsson, 1992). HB is a proton-donating group near the binuclear center (Hallén & Nilsson, 1992).

Scheme 1: Proposed Mechanism for the Reduction of Dioxygen to Water by Cytochrome *c* Oxidase

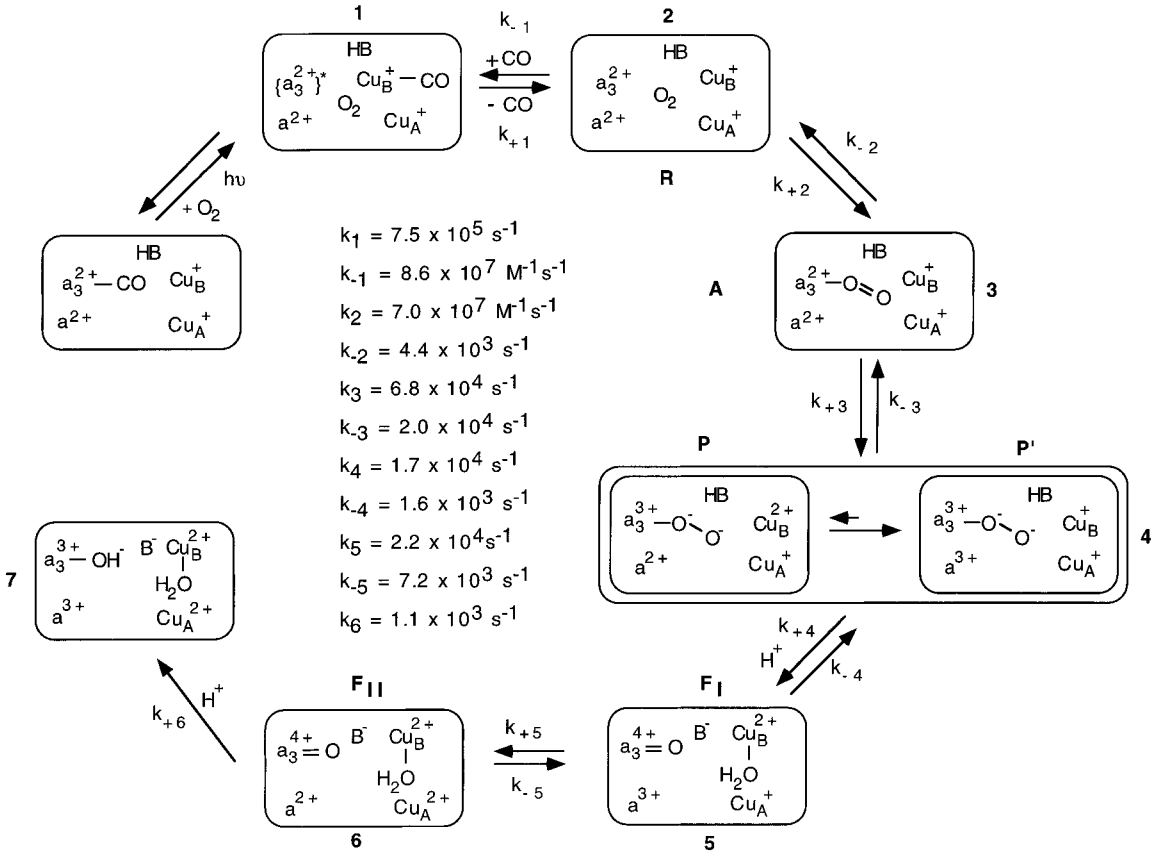

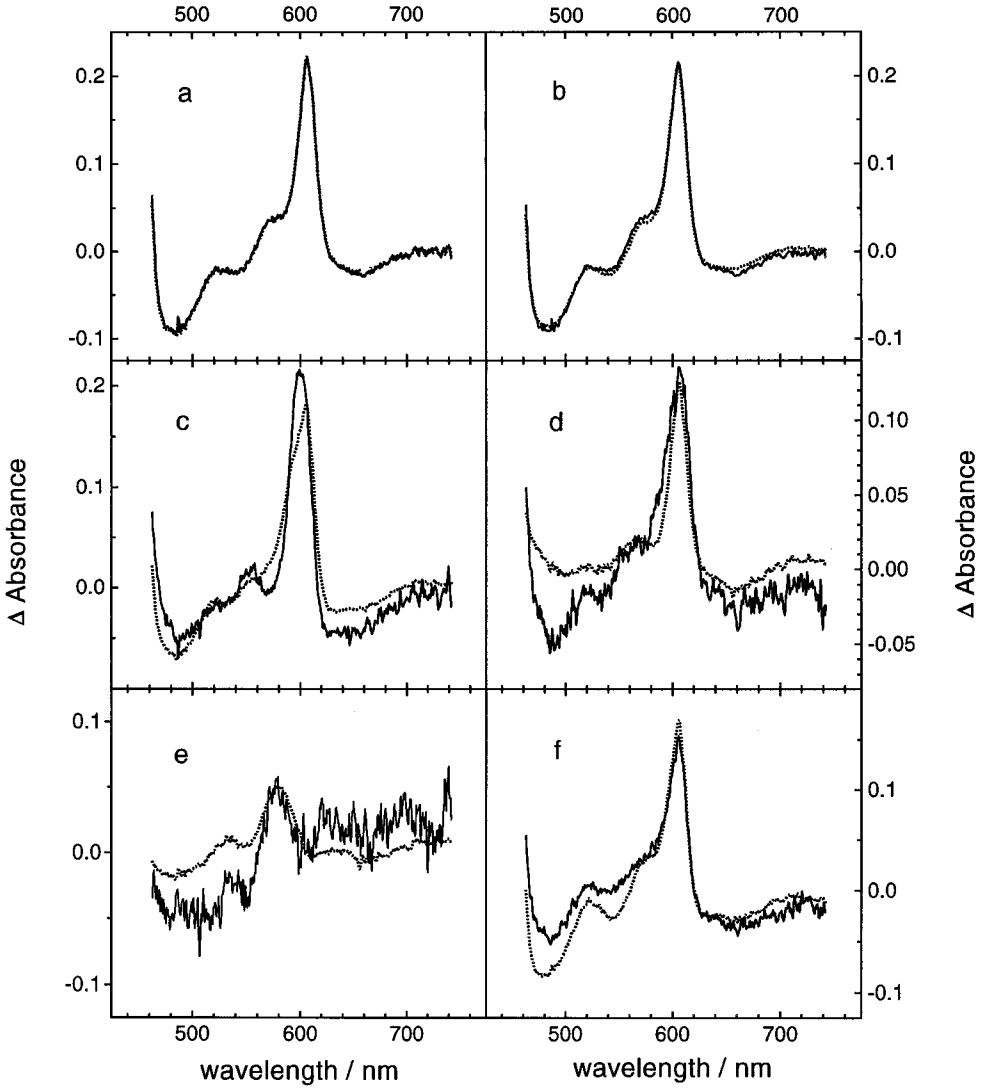

FIGURE 5: Comparison of the experimental (solid lines) and theoretical (dotted lines) difference spectra of the intermediates present during the reaction of the fully reduced enzyme with dioxygen (Scheme 1). The reference spectrum is that of the oxidized enzyme. The experimental difference spectra were determined on the basis of the mechanism and the microscopic rate constants in Scheme 1. The theoretical difference spectra were obtained by the appropriate linear combination of the ground-state spectra of the oxidized, reduced, mixed-valence CO, and fully reduced CO complexes and the peroxy and ferryl derivatives (see text for details). (Panels a−f) Experimental and theoretical difference spectra of intermediates 1−6.

Intermediate Absorption Difference Spectra. The difference spectra (referenced against the oxidized enzyme) of the intermediates (1−7) extracted from the original transient difference spectra using the mechanism and microscopic rate constants in Scheme 1 (experimental spectra) are shown in Figure 5 (solid lines). Figure 5 (dotted lines) shows the theoretical intermediate difference spectra for comparison.

In general, there is very good agreement between the experimental intermediate difference spectra and the theoretical difference spectra. The theoretical difference spectrum for intermediate 1 is the 50-ns spectrum (referenced against the oxidized enzyme) since we do not know the spectral profile of $\{a_3^{2+}\}^*$ (Figure 5a). The equilibrium constant for the first step, $K_1 = k_{-1}/k_1$, is equal to ~115 M^{-1}, a value consistent with that reported earlier for the fully reduced CO-bound enzyme in the absence of dioxygen (Einarsdóttir et al., 1995). There is excellent correspondence between the experimental difference spectrum of intermediate 2 and that of the theoretical difference spectrum (Figure 5b), the latter being the ground-state difference spectrum of the fully reduced enzyme.

The theoretical difference spectrum for intermediate 3, compound A, is the difference spectrum of the fully reduced CO complex, since we do not know the spectrum of compound A (Figure 5c). As shown below, the discrepancy between the experimental and the theoretical intermediate difference spectra is not due to bad fitting but simply reflects the fact that the spectrum of the ferrous-oxy complex is different from that of the CO complex. The O_2 on-rate is 7 × 10^7 M^{-1} s^{-1}, and the dissociation constant (k_{-2}/k_2 ~60 μM) is close to that reported by Orii (1988b).

Intermediate 4 represents a mixture of peroxy species (a_3^{3+}-O^--O^-) in which cytochrome *a* is reduced (P) and oxidized (P′) (Figure 5d, solid line). The theoretical difference spectrum of P′ is the difference spectrum of the species made by exposing a solution of the oxidized enzyme to CO in the presence of O_2 (Fabian & Palmer, 1995a). The theoretical difference spectrum of P was obtained by adding the reduced-minus-oxidized spectrum of cytochrome *a* (the difference spectrum of the fully reduced CO enzyme and the mixed-valence CO complex) to the theoretical difference spectrum of P′. The very good agreement between the

experimental and theoretical difference spectra of intermediate 4 (both showing a peak at 606 nm, Figure 5d) was obtained by assuming an equilibrium constant of 6 in favor of P′. The rate constant for the formation of intermediate 4 is 6.8×10^4 s^{-1}, a value similar to that reported by Hill (1994). However, in Hill's scheme, this step did not include a reverse rate constant, while in our simulation, a reverse rate constant of 2×10^4 s^{-1} is required to obtain the best fit between the experimental and theoretical difference spectra.

The conversion of the peroxy species to the ferryl species represented by intermediate 5, F_I, occurs with a forward rate constant of 1.7×10^4 s^{-1}. The spectrum of this intermediate has not been previously resolved at room temperature. There is good agreement between the experimental and theoretical difference spectra of F_I (Figure 5e). The theoretical difference spectrum of F_I was obtained by previously published procedures (Fabian & Palmer, 1995a). The experimental difference spectrum has a peak at ~578 nm, while the theoretical one has a maximum at 580 nm. The discrepancy between the experimental and theoretical difference spectra of F_I between 500 and 550 nm will be discussed below.

The formation of F_I is followed by a slightly faster ($k_5 + k_{-5} = 2.9 \times 10^4$ s^{-1}) electron redistribution between cytochrome *a* and Cu_A. This is in accordance with our observation from the double difference map (Figure 2), which showed that the electron transfer from Cu_A to cytochrome *a* (reflected by an increase at 605 and 520 nm) closely followed the formation of F (the increase at ~580 nm). There is good agreement between the experimental and theoretical difference spectra of intermediate 6, F_{II}, in which cytochrome a_3 is in its ~580-nm ferryl form, but cytochrome *a* is re-reduced (Figure 5f). Both the experimental and theoretical difference spectra have a maximum at 605 nm. The theoretical difference spectrum of F_{II} was obtained by adding the reduced-minus-oxidized spectrum of cytochrome *a* to the theoretical difference spectrum of F_I.

The discrepancy between the experimental and theoretical difference spectra of F_I between 500 and 550 nm (Figure 5e) stems from the fact that while the oxidation states of the two hemes are the same, the oxidation states of the coppers are not. The oxidation states of the hemes and coppers of F_I in Scheme 1 when referenced against the oxidized enzyme are $a_3^{4+}{=}O - a_3^{3+}$ and $Cu_A^{+} - Cu_A^{2+}$, while those of the theoretical difference spectrum are $a_3^{4+}{=}O - a_3^{3+}$. We have previously shown that Cu_A^{2+} has an absorbance spectrum with a maximum centered at ~520 nm (Einarsdóttir et al., 1995). Therefore, the lower absorbance in the region between 500 and 550 nm in the experimental difference spectrum of F_I compared to the theoretical spectrum is due to the negative contribution of Cu_A^{2+}. The same explanation applies to the discrepancy between the experimental and theoretical difference spectra of intermediates 4 and 6. For example, the oxidation states of the hemes and the coppers in F_{II} according to Scheme 1 (when referenced against the oxidized enzyme) are $a_3^{4+}{=}O - a_3^{3+}$ and $a^{2+} - a^{3+}$, while in the theoretical spectrum they are $a_3^{4+}{=}O - a_3^{3+}$, $a^{2+} - a^{3+}$, and $Cu_A^{+} - Cu_A^{2+}$. In this case the negative contribution of Cu_A^{2+} to the theoretical difference spectrum results in lower absorbance between 500 and 550 nm compared to the experimental spectrum (Figure 5f).

The difference spectrum of intermediate 7, the ferric hydroxide, is similar to that of the oxidized enzyme (the theoretical difference spectrum) but with slightly higher intensity at 600 nm (not shown). The formation of intermediate 7 is unidirectional with a rate constant of 1.1×10^3 s^{-1}, a value similar to those reported previously (Oliveberg et al., 1989; Hill, 1991).

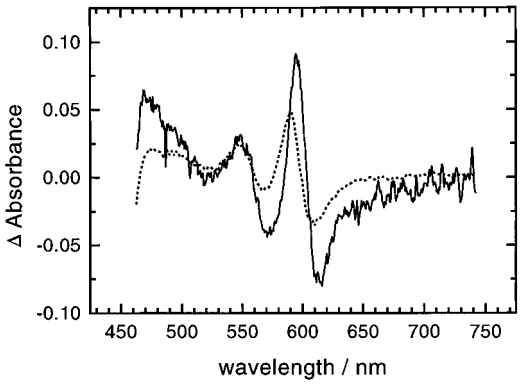

FIGURE 6: (Solid line) Difference between the experimental spectrum of intermediate 3, compound A, and intermediate 2, the fully reduced unliganded enzyme (Scheme 1), a_3^{2+}-O_2 minus a_3^{2+}. (Dotted line) Difference between the spectra of the fully reduced CO complex and the fully reduced unliganded enzyme, a_3^{2+}-CO minus a_3^{2+}.

To further establish that the difference spectra in Figure 5 reflect those of the intermediates depicted in Scheme 1, we have compared the experimental spectral differences between successive intermediates to the theoretical differences. Figure 6 (solid line) shows the difference between compound A (intermediate 3) and the fully reduced enzyme (intemediate 2), a_3^{2+}-$O_2 - a_3^{2+}$. The analogous difference spectrum of the fully reduced CO-bound complex is shown for comparison (Figure 6, dotted line). The experimental difference spectrum of compound A has a peak at 595 nm and a trough at 612 nm, values similar to those observed at low temperature (Chance et al., 1975; Clore et al., 1980) and at room temperature for the mixed-valence enzyme (Hill & Greenwood, 1983). The ferrous-oxy complex has been observed for the fully reduced enzyme by TR^3 spectroscopy (Varotsis et al., 1989; Ogura et al., 1990a; Han et al., 1990b), and recent transient optical absorption studies have provided evidence for this intermediate at −25 °C (Morgan et al., 1996). Its existence at room temperature has been inferred on the basis of transient optical absorption measurements (Orii, 1984, Orii, 1988a,b; Oliveberg et al., 1989; Hill, 1994; Verkhovsky et al., 1994). However, the optical difference spectrum of compound A has not been previously reported, and Figure 6 (solid line) unequivocally shows its difference spectrum at room temperature. The significantly higher intensity and red shift of the difference spectrum compared to that of the CO complex have also been observed at low temperature for the mixed-valence enzyme (Clore, 1980) and are consistent with model studies (Babcock & Chang, 1979).

The oxidation states of the hemes in the difference spectrum of intermediate 4 (Figure 5d), the two peroxy species P and P′ in a 1:6 ratio, are a_3^{3+}-O^--$O^- - a_3^{3+}$ (100%) and $a^{2+} - a^{3+}$ (15%). For simplicity the oxidation states of the coppers are omitted. To get the difference spectrum of cytochrome a_3 alone, i.e., that of P′, we subtracted the contribution of the reduced-minus-oxidized difference spectrum of cytochrome *a* from the difference spectrum in Figure 5d (solid line). The resulting difference spectrum shown in Figure 7a is a_3^{2+}-O^--$O^- - a_3^{3+}$. Both the experimental and the theoretical difference spectra have a peak at 606 nm,

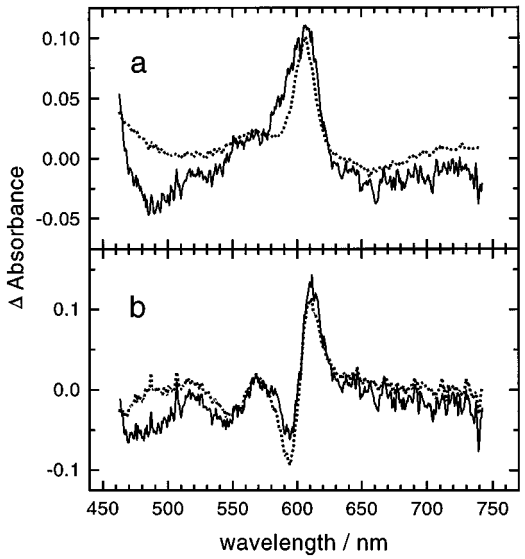

FIGURE 7: (a) Experimental (solid line) and theoretical (dotted line) difference between intermediates 4 and 3 after the contribution (15%) of the reduced-minus-oxidized difference spectrum of cytochrome *a* has been subtracted. The oxidation states of the hemes and coppers in the resulting experimental difference spectrum (the difference spectrum of P′) are: a_3^{2+}-O^--O^- − a_3^{3+}, Cu_B^+ − Cu_B^{2+}, Cu_A^+ − Cu_A^{2+}, and a_3^{2+}-O^--O^--a_3^{3+} in the case of the theoretical difference spectrum. (b) (Solid line) Difference spectrum between the experimental difference spectra of intermediate 4 (Figure 5d, solid line) and compound A (Figure 5c, solid line) after the contribution (85%) of the oxidized-minus-reduced difference spectrum of cytochrome *a* has been subtracted. The resulting experimental and "theoretical" difference spectra are a_3^{2+}-O^--O^- − a_3^{2+}-O═O, Cu_B^{2+} − Cu_B^+. The "theoretical" difference spectrum is equal to the difference between the theoretical spectrum of P and the experimental spectrum of compound A.

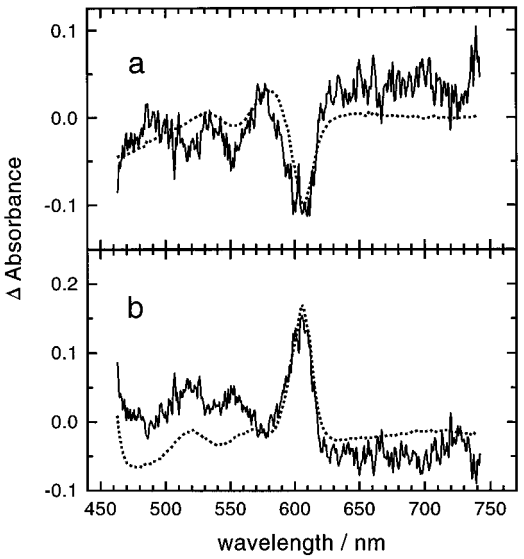

FIGURE 8: Experimental (solid line) and theoretical (dotted line) difference between intermediate 5 (F_I) and P′. This corresponds to a_3^{4+}═O − a_3^{3+}-O^--O^-, Cu_B^{2+} − Cu_B^+ in the case of the experimental difference spectrum and a_3^{4+}─O − a_3^{3+}-O^--O^- in the case of the theoretical one. (B) Experimental (solid line) and theoretical (dotted line) difference between intermediates 6 (F_{II}) and 5 (F_I). The resulting experimental difference spectrum (solid line) corresponds to a^{2+} − a^{3+}, Cu_A^{2+} − Cu_A^+ and the theoretical difference is a^{2+} − a^{3+}, Cu_A^+ − Cu_A^{2+}.

analogous to compound C observed at low temperature (Chance et al., 1975), but the experimental difference spectrum has a slightly larger bandwidth. The discrepancy between the experimental and theoretical difference spectra in the 500−550-nm region is, as discussed above, due to the negative contribution of Cu_A^{2+} to the experimental spectrum.

The difference spectrum between intermediate 4 (Figure 5d, solid line) and compound A (Figure 5c, solid line), a_3^{2+}-O^--O^- − a_3^{2+}-O═O (100%), a^{3+} − a^{2+} (85%), has a contribution from both cytochromes a_3 and *a*. Figure 7b (solid line) shows the peroxy-minus-compound A (P minus A) difference spectrum of cytochrome a_3 (a_3^{2+}-O^--O^- − a_3^{2+}-O═O) obtained after subtracting the contribution of the oxidized-minus-reduced difference spectrum of cytochrome *a* from the difference spectrum between intermediate 4 and compound A. Figure 7b (dotted line) shows the corresponding "theoretical" difference spectrum which was obtained by subtracting the experimental difference spectrum of compound A (Figure 6, solid line) from the theoretical difference spectrum of P. The peaks and troughs are at 611 and 594 nm, respectively, in both the experimental and the theoretical difference spectra (Figure 7b). Therefore, the peak at 607 nm in the spectrum of the cytochrome a_3 when referenced against the oxidized cytochrome a_3 is shifted to 611 nm when the reference is the ferrous-oxy complex. The peak and trough values of 611 and 594 nm are consistent with the values (610 and 595 nm) observed for the analogous difference spectrum of the final product formed during the reaction of the mixed-valence enzyme with dioxygen (Hill & Greenwood, 1983). This product was attributed to a peroxy species. The good agreement between the experimental and theoretical difference spectra in Figure 7 provides conclusive evidence for the conversion of compound A to a peroxy species in the reaction of the fully reduced enzyme with dioxygen.

Figure 8a (solid line) shows the difference between the difference spectra of intermediate 5, F_I, a_3^{4+}═O − a_3^{3+} (Figure 6e, solid line), and intermediate 4, a_3^{3+}-O^--O^- − a_3^{3+} (100%), a^{2+} − a^{3+} (15%) (Figure 6d, solid line), after the contribution (15%) of the reduced-minus-oxidized cytochrome *a* has been added. The resultant experimental difference spectrum, F_I − P′, ferryl-minus-peroxy, a_3^{4+}═O − a_3^{3+}-O^--O^-, has a peak at 575 nm and a trough at ∼607 nm reflecting the conversion of the peroxy form to the ferryl form. The corresponding theoretical difference spectrum, the difference between F (580-nm absorbance maximum) and the peroxy form (607-nm absorbance maximum) shows a peak at 582 nm and a trough at 607 nm. The good agreement between the experimental and theoretical difference spectra provides further support for the assignments in Scheme 1. The difference between the experimental and theoretical spectra of intermediate 4 (Figure 6d) and intermediate 5 (Figure 6e) in the region between 500 and 550 nm (the Cu_A^{2+} contribution) cancels out in the double difference spectrum (Figure 8a).

The experimental difference between the two ferryl species, F_{II} minus F_I (Figure 6, spectra f minus e, solid lines) is shown in Figure 8b (solid line). According to Scheme 1, this difference should equal the reduced-minus-oxidized spectrum of cytochrome *a* and the oxidized-minus-reduced spectrum of Cu_A, a^{2+} − a^{3+} and Cu_A^{2+} − Cu_A^+. The excellent agreement between this difference spectrum and the theoretical cytochrome *a* reduced-minus-oxidized difference spectrum, a^{2+} − a^{3+} and Cu_A^+ − Cu_A^{2+} (Figure 8b, dotted line), strongly argues for the presence of two ferryl

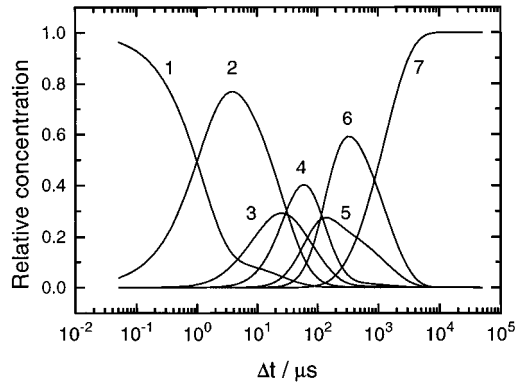

FIGURE 9: Relative concentration−time profiles of the intermediates present during the reaction of the fully reduced enzyme with dioxygen. The time profiles are based on the mechanism and microscopic rate constants in Scheme 1.

species in the oxygen-reduction pathway. As discussed above, the discrepancy between the experimental and the theoretical difference spectra between 500 and 550 nm is due to the different redox states of Cu_A in the two spectra.

Time−Concentration Profiles. On the basis of the mechanism and the microscopic rate constants in Scheme 1, we can simulate the time course of the dioxygen reduction reaction to determine the relative time−concentration profiles of the various intermediates. These are shown in Figure 9. The time profile for compound A (intermediate 3) shows that this species has a very short lag phase (50 ns−1 μs) and reaches its maximum concentration ~30 μs following photolysis, in agreement with the second **uv** couple and the double difference map. Intermediate 4 (the mixture of the two peroxy species) reaches its maximum concentration ~60 μs after photolysis, at which time compound A has decayed to ~75% of its concentration. These time profiles are consistent with previous optical and TR[3] studies which indicated that the oxidation of cytochrome *a* occurs with an apparent rate constant of 3×10^4 s^{-1}, coinciding with the decay of the oxy complex (Han et al., 1990c; Hill, 1994; Verkhovsky et al., 1994). However, neither peroxy species represented by intermediate 4 in Scheme 1 has been detected by resonance Raman spectroscopy.

The formation of the peroxy species is followed by the formation of the first ferryl, F_I (Scheme 1). The time scale of the cleavage of the O−O bond to produce a ferryl has been somewhat uncertain. There is agreement that a resonance mode observed between 300 μs and 1.5 ms at 786 cm^{-1} can be assigned to a_3^{4+}═O (Varotsis & Babcock, 1990; Han et al., 1990a; Ogura et al., 1990b). However, Orii (1988a) attributed peaks at 575 and 530 nm in the 100-μs minus 20-μs optical absorption difference spectrum observed during the reaction of the fully reduced enzyme with dioxygen to the formation of F. The formation of F_I occurs on a similar, but not identical, time scale as the subsequent electron redistribution between cytochrome *a* and Cu_A (Figure 9). In fact, only by assuming that the latter process occurs on a faster time scale ($k_5 + k_{-5} = 2.9 \times 10^4$ s^{-1}) than the former ($k_4 + k_{-4} = 1.9 \times 10^4$ s^{-1}) was it possible to obtain the spectrum of F_I. The time profiles in Figure 9 show that the two ferryl species reach a maximum concentration at ~310 μs after photolysis, at which time compound A and the peroxy intermediates have nearly disappeared, and the last intermediate has started to form. This is in accordance with our previous interpretation of the double difference map and the third **uv** couple. A species with a resonance Raman frequency at 804 cm^{-1} has been observed by Ogura et al. (1996) prior to the formation of the 785-cm^{-1} species. The 804-cm^{-1} mode was assigned to a_3^{5+}═O (Cu_B^{2+}) which is formally at the oxidation state of a peroxide, and the authors suggested that this species followed the formation of compound A. However, this frequency has not been detected by either Han and Rousseau or Varotsis and Babcock. The discrepancy between the groups has been attributed to differences in the way time resolution is achieved, as well as different O_2 concentrations employed (Varotsis et al., 1993). In view of Scheme 1, we tentatively assign the 804-cm^{-1} mode to F_I and the 785-cm^{-1} mode to F_{II}, although it is unclear whether a redox state change in cytochrome *a* could cause a 20-cm^{-1} shift in the Fe═O stretch.

The last species in Scheme 1, the ferric hydroxide, reaches half its maximum concentrsation at ~1 ms. This is consistent with TR[3] results in which a resonance Raman mode observed at 450 cm^{-1} between 500 μs and 2 ms after photolysis was assigned to the ferric hydroxide (Han et al., 1990a; Varotsis et al., 1993).

Structure of the Peroxy and the Ferryl. The structures of the two species with absorbance maxima at ~607 and ~580 nm when referenced against the oxidized enzyme and normally attributed to a peroxy (a_3^{3+}-O^--O^-) and a ferryl (a_3^{4+}═O), respectively, are uncertain (Proshlyakov et al., 1994; Fabian & Palmer, 1995b). While our data reveal the optical spectroscopic signatures of the intermediates present during the dioxygen reduction cycle, they cannot tell unequivocally what the actual structures are. Resonance Raman spectra give structural information, but as mentioned above, there is no consensus regarding assignments or time scales of some of the intermediates. There appears to be agreement that the resonance mode at 785 cm^{-1} observed between 300 μs and 1.5 ms after photolysis is due to a_3^{4+}═O (Cu_B^{2+}), which according to our time profiles most likely is F_{II}. In reverse electron transfer experiments, Wikström (1992) observed two species with maxima at 580 and 607 nm in the difference spectra referenced against the oxidized enzyme, which he assigned to F (a_3^{4+}═O) and P (a_3^{3+}-O^--O^-), respectively. Using evidence from EPR and optical absorption, Witt and co-workers proposed that a three-electron-reduced dioxygen intermediate with a maximum at 580 nm when referenced against the oxidized enzyme was a ferryl (Witt et al., 1986; Witt & Chan, 1987).

As shown above, cytochrome a_3 has the same electronic structure in both P and P′, giving rise to a peak at ~606 nm in the difference spectrum referenced against the oxidized enzyme. One possible structure of cytochrome a_3 in both species would be the peroxy structure indicated in Scheme 1, a_3^{3+}-O^--O^-. As mentioned earlier, it is not unlikely that the peroxide is bridging between cytochrome a_3 and Cu_B. In P′, one more electron equivalent resides in the binuclear center, on Cu_B, compared to P. A second alternative is that both species have cytochrome a_3 in its ferryl state, a_3^{4+}═O, with an oxidizing equivalent in P on Cu_B (Cu_B^{3+}) (Fabian & Palmer, 1995b) or on an amino acid radical or porphyrin π-cation radical. However, as recently suggested by Morgan et al. (1996), if P had the a_3^{4+}═O Cu_B^{3+} structure, then P′ with one more reducing equivalent would be a_3^{4+}═O Cu_B^{2+}, which according to TR[3] is the structure of F. This would be inconsistent with our data above, which show that

cytochrome a_3 has the same spectrum in P′ and P, different from that of F. On the basis of magnetic circular dichroism data, Fabian and Palmer (1995b) have recently shown that an a_3^{4+}═O structure with a porphyrin cation radical is not feasible. This has been supported by TR^3 experiments (Proshlyakov et al., 1996). It is possible that both P and P′ have the a_3^{4+}═O Cu_B^{2+} structure, with an amino acid radical as the source of the extra oxidizing equivalent in P′. However, both Palmer and Witström have provided arguments against this assignment (Fabian & Palmer, 1995b; Morgan et al., 1996). A third possibility recently proposed for the structure of P is a_3^{5+}═O Cu_B^{2+} (Ogura et al., 1996), and the resonance Raman line at 804 cm^{-1} has been attributed to this structure. Again, if P had the a_3^{5+}═O and Cu_B^{2+} structure, then P′ with one more reducing equivalent would most likely be a_3^{4+}═O Cu_B^{2+} (i.e., F), which is inconsistent with our data. Therefore, we favor the structures shown in Scheme 1 for the P, P′, and F intermediates.

Proshlyakov et al. (1994) have recently shown that the 804-cm^{-1} mode can be observed when a "607-nm form" of cytochrome oxidase (obtained upon addition of hydrogen peroxide to the resting enzyme) is excited at 607 nm. Using $^{16}O-^{18}O$ mixed isotopes, the authors showed that the 804-cm^{-1} species was due to a ferryl and not a peroxide. The authors also found that the intensity of the Raman scattering became weaker when the excitation wavelength was moved to 580 nm. On the basis of these observations, the authors assigned the 804-cm^{-1} mode to the 607-nm species. However, as pointed out by Fabian and Palmer (1995b), the 580-nm excited scattering would appear at 607 nm and the 607-nm scattering at 638 nm. Thus, the greater self-absorption in the case of the 580-nm excitation could account for the weakening of the 804-cm^{-1} mode at this excitation wavelength. This, combined with the observation that the difference spectrum of the "607-nm form" reported by Proshlyakov et al. (1994) appears to have a mixture of the 607- and 580-nm species (in a ratio of approximately 70:30), does not exclude the 580-nm species as being responsible for the 804-cm^{-1} mode. It should also be noted that the excitation wavelengths of 607 and 580 nm are the maxima of the "peroxy" and "ferryl" species when referenced against the oxidized enzyme but not those of the cytochrome a_3 species alone. When the spectrum of the oxidized enzyme is added to their difference spectra, the "peroxy" and "ferryl" species have maxima at 599 and 605 nm, respectively, suggesting that either species could be excited at 607 nm. Excitation profiles of the pure 607-nm complex could help determine the structure of this species.

CONCLUSIONS

The optical data presented above show for the first time the difference spectra of compound A and the peroxy and ferryl species present during the reduction of dioxygen to water at room temperature. The time profiles unequivocally establish the time scales on which these species are formed. According to our modeling, the two peroxy species are formed prior to the ferryl, and the excellent agreement between the experimental and theoretical difference spectra of the intermediates (Figures 5, 7, and 8) supports this.

Our model also establishes that the two peroxy species, P and P′, are formed in a ratio of 1:6. It is important to note that, in both species, cytochrome a_3 has a peak at 606 nm when referenced versus its oxidized form (Figure 7a, solid line), and its difference spectrum is quite similar to the spectrum obtained upon exposing the fully oxidized enzyme to CO in the presence of dioxygen (Figure 7b, dotted line), indicating that the two species are the same. The spectral similarities between the peroxy species observed here, compound C at low temperature (Chance et al., 1975), and the final product observed during the reaction of dioxygen with the mixed-valence enzyme at room temperature (Hill & Greenwood, 1983; Han et al., 1990d) provide convincing arguments that all three are the same.

The two peroxy species have not been detected previously at room temperature in the catalytic cycle of the reduced enzyme, either by optical or resonance Raman spectroscopy, although P′ was recently observed in transient optical measurements at −25 °C (Morgan et al., 1996). Indeed, there has been considerable debate whether intermediate P is a true intermediate in the dioxygen redcuction cycle [see Einarsdóttir et al. (1995) for review]. We have previously shown that, upon flash photolysis of the mixed-valence CO enzyme in the absence of dioxygen, the rate constant for the electron transfer from cytochrome *a* to cytochrome a_3 is $\sim 1.8 \times 10^5$ s^{-1} (Einarsdóttir et al., 1995), a value similar to that obtained by other groups (Oliveberg & Malmström, 1991; Verkhovsky et al., 1992). The equilibrium constant of 6 between the two peroxy species is identical to the ratio of the rate constant for the electron transfer from cytochrome *a* and cytochrome a_3, 1.8×10^5 s^{-1}, and the apparent rate constant for the decay of compound A and oxidation of cytochrome *a*, 3×10^4 s^{-1}, observed here and reported previously (Han et al., 1990c; Hill, 1994; Verkhovsky et al., 1994). This indicates that the peroxy species, P, is formed upon decay of the oxy complex with a rate constant of 3×10^4 s^{-1} but is rapidly converted to the P′ form upon fast electron transfer between the cytochrome *a* and the binuclear center as proposed earlier (Verkhovsky et al., 1992). The small population of P would account for the fact that it has not been detected in the resonance Raman spectra and optical absorption spectra. Although we have not resolved the two peroxy species, we have shown that the observed spectrum of intermediate 4 (Figure 5d, solid line) resembles the theoretical spectrum only if one assumes that the two species are formed in a ratio of 1:6. Thus our data demonstrate that both P and P′ are indeed intermediates in the reaction of the fully reduced enzyme with dioxygen at room temperature.

Our data also establish that there are two ferryl species on the route from dioxygen to water, F_I and F_{II} in which cytochrome *a* is oxidized and reduced, respectively. The presence of a ferryl compound in the reaction of the fully reduced enzyme with dioxygen was suggested based upon the observation of a 575-nm peak in the 100-μs minus 20-μs flow-flash difference spectrum (Orii, 1988a), and recent optical absorption studies have provided evidence for F_{II} at −25 °C (Morgan et al., 1996).

The similarities between the experimental and theoretical difference spectra of both the peroxy and the ferryl species (Figures 5d−f, 7, and 8) make it highly likely that the intermediates in the dioxygen reduction cycle are the same as those obtained upon adding hydrogen peroxide (F) and a mixture of CO and O_2 (P) to the oxidized enzyme. This is supported by recent TR^3 experiments (Proshlyakov et al., 1996) in which the same modes were observed upon the addition of hydrogen peroxide to the oxidized enzyme as

those detected during the reaction of the fully reduced enzyme with dioxygen.

REFERENCES

Alben, J. O., Moh, P. P., Fiamingo, F. G., & Altschuld, R. A. (1981) *Proc. Natl. Acad. Sci. U.S.A. 78*, 234−237.

Antalis, T. M., & Palmer, G. (1982) *J. Biol. Chem. 257*, 6194−6206.

Babcock, G. T., & Chang, C. K. (1979) *FEBS Lett. 97*, 358−362.

Babcock, G. T., & Wikström, M. (1992) *Nature 356*, 301−309.

Bailey, J. A., James, C. A., & Woodruff, W. H. (1996) *Biochem. Biophys. Res. Commun. 220*, 1055−1060.

Bickar, D., Bonaventura, J., & Bonaventura, C. (1982) *Biochemistry 21*, 2661−2666.

Blackmore, R. S., Greenwood, C., & Gibson, Q. H. (1991) *J. Biol. Chem. 266*, 19245−19249.

Blair, D. F., Witt, S. N., & Chan, S. I. (1985) *J. Am. Chem. Soc. 107*, 7389−7399.

Chance, B., Saronio, C., & Leigh, J. S., Jr. (1975) *J. Biol. Chem. 250*, 9226−9237.

Clore, G. M. (1980) *Biochem. J. 187*, 617−622.

Clore, G. M., Andréasson, L.-E., Karlsson, B. G., Aasa, R., & Malmström, B. (1980) *Biochem. J. 185*, 139−154.

Dyer, R. B., Einarsdóttir, Ó., Killough, P. M., López-Garriga, J. J., & Woodruff, W. H. (1989) *J. Am. Chem. Soc. 111*, 7657−7659.

Einarsdóttir, Ó. (1995) *Biochim. Biophys. Acta 1229*, 129−147.

Einarsdóttir, Ó., Dyer, R. B., Lemon, D. D., Killough, P. M., Hubig, S. M., Atherton, S. J., López-Garriga, J. J., Palmer, G., & Woodruff, W. H. (1993) *Biochemistry 32*, 12013−12024.

Einarsdóttir, Ó., Georgiadis, K. E., & Sucheta, A. (1995) *Biochemistry 34*, 496−508.

Fabian, M., & Palmer, G. (1995a) *Biochemistry 34*, 1534−1540.

Fabian, M., & Palmer, G. (1995b) *Biochemistry 34*, 13802−13810.

Georgiadis, K. E., Jhon, N.-I., & Einarsdóttir, Ó. (1994) *Biochemistry 33*, 9245−9256.

Gibson, Q. H., & Greenwood, C. (1963) *Biochem. J. 86*, 541−554.

Golub, G. H., & Reinsch, C. (1970) *Numer. Math. 14*, 403−420.

Greenwood, C., & Gibson, Q. H. (1967) *J. Biol. Chem. 242*, 1782−1787.

Hallén, S., & Nilsson, T. (1992) *Biochemistry 31*, 11853−11859.

Han, S., Ching, Y.-C., & Rousseau, D. L. (1990a) *Nature 348*, 89−90.

Han, S., Ching, Y.-C., & Rousseau, D. L. (1990b) *Proc. Natl. Acad. Sci. U.S.A. 87*, 2491−2495.

Han, S., Ching, Y.-C., & Rousseau, D. L. (1990c) *Proc. Natl. Acad. Sci. U.S.A. 87*, 8408−8412.

Han, S., Ching, Y.-C., & Rousseau, D. L. (1990d) *J. Am. Chem. Soc. 112*, 9445−9451.

Hannsson, Ö., Karlsson, B., Aasa, R., Vänngård, T., & Malmström, B. G. (1982) *EMBO J. 1*, 1295−1297.

Henry, E. R., & Hofrichter, J. (1992) *Methods Enzymol. 210*, 129−193.

Hill, B. C. (1991) *J. Biol. Chem. 266*, 2219−2226.

Hill, B. C. (1994) *J. Biol. Chem. 269*, 2419−2425.

Hill, B. C., & Greenwood, C. (1983) *Biochem. J. 215*, 659−667.

Hill, B. C., & Greenwood, C. (1984) *Biochem. J. 218*, 913−921.

Hug, S. J., Lewis, J. W., Einterz, C. M., Thorgeirsson, T. E., & Kliger, D. S. (1990) *Biochemistry 29*, 1475−1485.

Karlsson, B., Aasa, R., Vänngård, T., & Malmström, B. G. (1981) *FEBS Lett. 131*, 186−188.

Morgan, J. E., Verkhovsky, M. I., & Wikström, M. (1996) *Biochemistry 35*, 12235−12240.

Ogura, T., Takahashi, S., Shinzawa-Itoh, K., Yoshikawa, S., & Kitagawa, T. (1990a) *J. Am. Chem. Soc. 112*, 5630−5631.

Ogura, T., Takahashi, S., Shinzawa-Itoh, K., Yoshikawa, S., & Kitagawa, T. (1990b) *J. Biol. Chem. 265*, 14721−14723.

Ogura, T., Takahashi, S., Hirota, S., Shinzawa-Itoh, K., Yoshikawa, S., Appleman, E. H., & Kitagawa, T. (1993) *J. Am. Chem. Soc. 115*, 8527−8536.

Ogura, T., Hirota, S., Proshlyakov, D. A., Shinzawa-Itoh, K., Yoshikawa, S., & Kitagawa, T. (1996) *J. Am. Chem. Soc. 118*, 5443−5449.

Oliveberg, M., & Malmström, B. G. (1991) *Biochemistry 30*, 7053−7057.

Oliveberg, M., & Malmström, B. G. (1992) *Biochemistry 31*, 3560−3563.

Oliveberg, M., Brzezinski, P., & Malmström, B. G. (1989) *Biochim,. Biophys. Acta 977*, 322−328.

Oliveberg, M., Hallén, S., & Nilsson, T. (1991) *Biochemistry 30*, 436−440.

Orii, Y. (1984) *J. Biol. Chem. 259*, 7187−7190.

Orii, Y. (1988a) *Ann. N.Y. Acad. Sci. 550*, 105−117.

Orii, Y. (1988b) *Chem. Scr. 28A*, 63−69.

Proshlyakov, D. A., Ogura, T., Shinzawa-Itoh, K., Yoshikawa, S., Appelman, E. H., & Kitagawa, T. (1994) *J. Biol. Chem. 269*, 29385−29388.

Proshlyakov, D. A., Ogura, T., Shinzawa-Itoh, K., Yoshikawa, S., & Kitagawa, T. (1996) *Biochemistry 35*, 76−82.

Thorgeirsson, T. E., Milder, S. J., Miercke, L. J. W., Betlach, M. C., Shand, R. F., Stroud, R. M., & Kliger, D. S. (1991) *Biochemistry 30*, 9133−9142.

Thorgeirsson, T. E., Lewis, J. W., Wallace-Williams, S. E., & Kliger, D. S. (1992) *Photochem. Photobiol. 56*, 1135−1144.

Varotsis, C., & Babcock, G. T. (1990) *Biochemistry 29*, 7357−7362.

Varotsis, C. A., & Babcock, G. T. (1995) *J. Am. Chem. Soc. 117*, 11260−11269.

Varotsis, C., Woodruff, W. H., & Babcock, G. T. (1989) *J. Am. Chem. Soc. 111*, 6439−6440.

Varotsis, C., Zhang, Y., Appleman, E. H., & Babcock, G. T. (1993) *Proc. Natl. Acad. Sci. U.S.A. 90*, 237−241.

Verkhovsky, M. I., Morgan, J. E., & Wikström, M. (1992) *Biochemistry 31*, 11860−11863.

Verkhovsky, M. I., Morgan, J. E., & Wikström, M. (1994) *Biochemistry 33*, 3079−3086.

Vygodina, T. V., & Konstantinov, A. A. (1988) *Ann. N.Y. Acad. Sci. 550*, 124−138.

Wikström, M., & Morgan, J. E. (1992) *J. Biol. Chem. 267*, 10266−10273.

Witt, S. N., & Chan, S. I. (1987) *J. Biol. Chem. 262*, 1446−1448.

Witt, S. N., Blair, D. F., & Chan, S. I. (1986) *J. Biol. Chem. 261*, 8104−8107.

Woodruff, W. H., Einarsdóttir, Ó., Dyer, R. B., Bagley, K. A., Palmer, G., Atherton, S. J., Goldbeck, R. A., Dawes, T. D., & Kliger, D. S. (1991) *Proc. Natl. Acad. Sci. U.S.A. 88*, 2588−2592.

Wrigglesworth, J. M. (1984) *Biochem. J. 217*, 715−719.

Yoshikawa, S., Choc, M. G., O'Toole, M. C., & Caughey, W. S. (1977) *J. Biol. Chem. 252*, 5498−5508.

BI962422K